

Supporting Information

**Stretchable and super-robust graphene superhydrophobic composite  
for electromechanical sensor application**

Peng Wang<sup>1</sup>, Bo Sun<sup>1</sup>, Ying Liang<sup>2</sup>, Huilong Han<sup>1</sup>, Xiaoliang Fan<sup>1</sup>, Wenliang Wang<sup>1</sup>, and Zhan Yang<sup>3</sup>

<sup>1</sup>School of Energy, Power and Mechanical Engineering, North China Electric Power University, Baoding, 071003, China

<sup>2</sup>State Key Lab of New Energy Power System, North China Electric Power University, 071003, Baoding, China

<sup>3</sup>Jiangsu Provincial Key Laboratory of Advanced Robotics & Collaborative Innovation Center Suzhou Nano Science and Technology, Soochow University

\*Corresponding author: wang.peng.ncepu@foxmail.com, yangzhan@suda.edu.cn

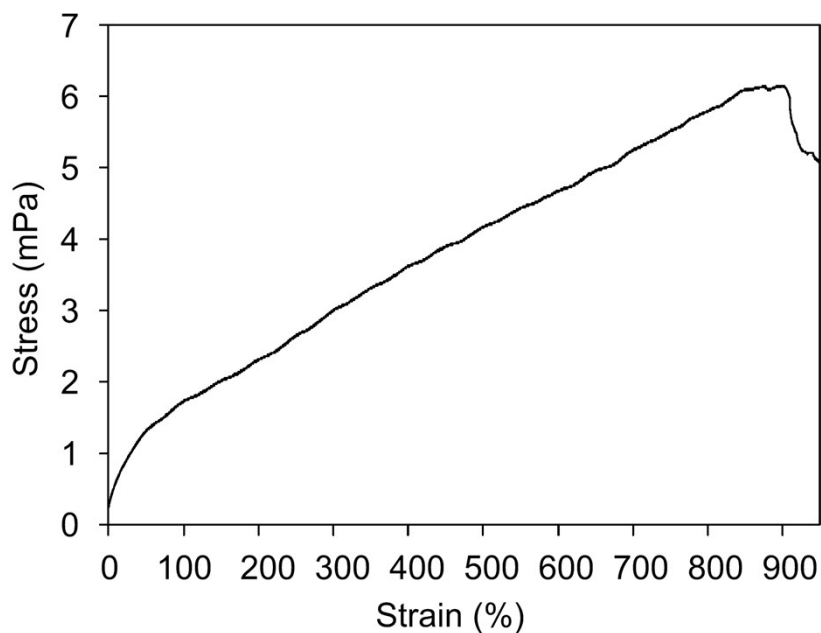


**Figure S1. Stress-strain curves of the graphene superhydrophobic composite.**

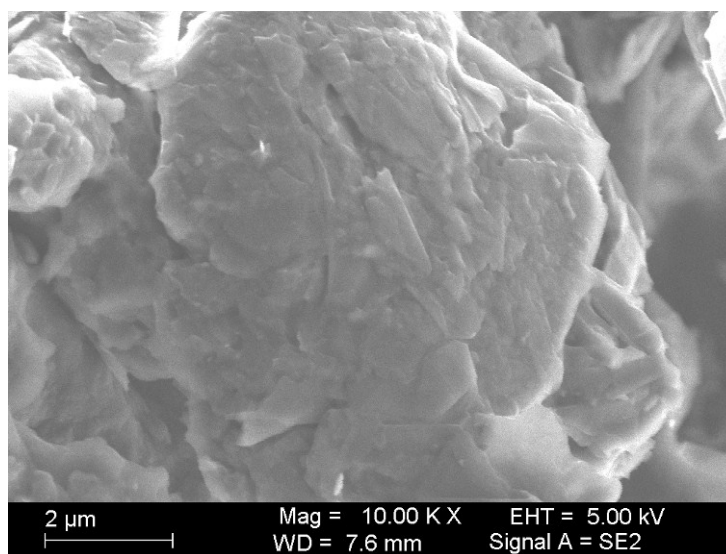


**Figure S2. High resolution SEM image from a part of SEM image in Figure 2a.**

### S3 XPS measurement

The surface chemical composition of the graphene superhydrophobic composite was analyzed by XPS (Thermo ESCALAB 250XI, USA) at room temperature, and the binding energies were calibrated with respect to the signal for adventitious carbon (284.8 eV). As shown in Figure S3a, the Si 2p, C 1s, O 1s and F 1s peaks are detected from the survey spectra of the sample. Curve-fitted F 1s core-level spectra of the sample are displayed in Figure S6b. The F1s peak in both cases was

observed at 688.42 eV, which corresponds to fluorine bonded as  $CF_x$  in the FAS chain indicating that F is present in same bonding environment as that of FAS [1-3]. Figure S3c shows the curve-fitted Si 2p spectra. The Si 2p core-level spectra shows a dominant peak at 103.20 eV, which could be due to  $SiO_2$ -based network [4,5]. Low-intense component peak around 104.54 eV corresponds to  $-Si-OH$  or  $Si-F_x$  species [6]. Fig. S6d shows the multi-element spectra of C 1s, observed peaks at 284.00, 284.84, 286.14, 289.05, 291.35 and 293.53 eV are ascribed to C-Si, C-C, C-O, C-CF,  $CF_2$  and  $CF_3$ , respectively [2,7,8].

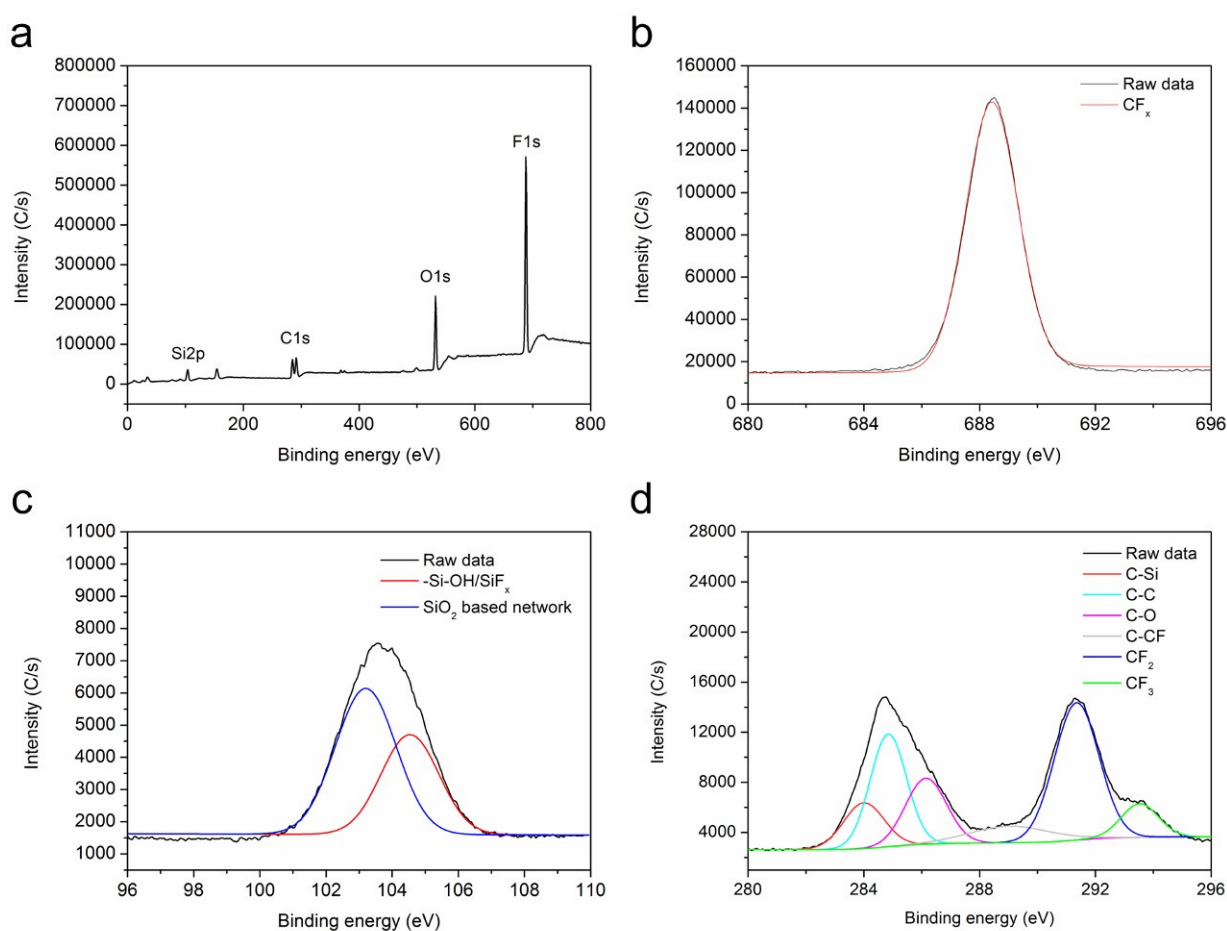


**Figure S3. XPS measurement of the graphence superhydrophobic composite.** (a) Survey XPS spectrum of the as-prepared superhydrophobic surface; (b) F 1s, (c) Si 2p and (d) C 1s XPS spectrum of the sample.



**Figure S4.** The picture of the graphene composite prepared without pre-stretch process.

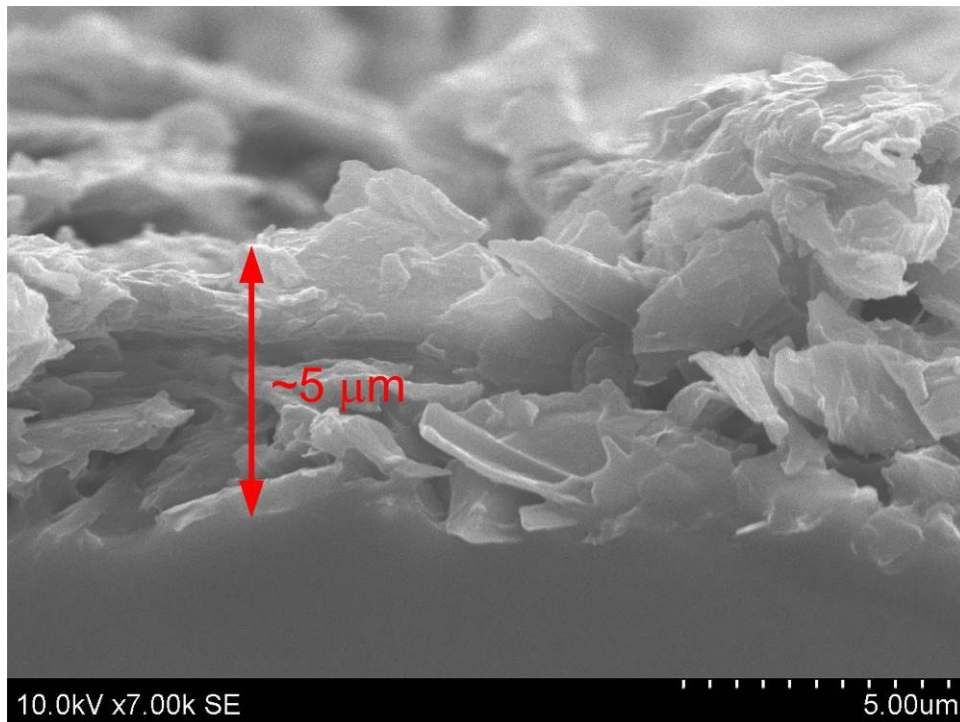


**Figure S5.** Cross-sectional SEM images of the graphene superhydrophobic composite.

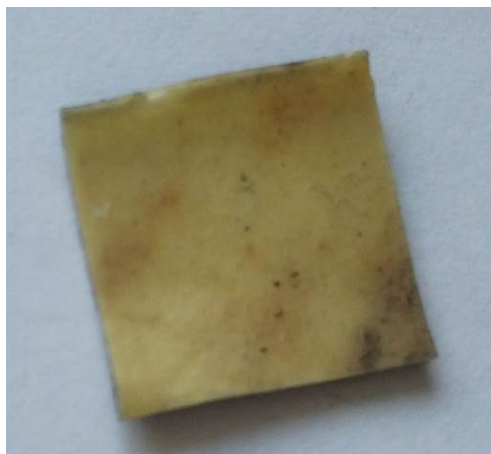


**Figure S6.** The picture of the graphene composite after treatment at 200 °C for 2h.

### S7 Reversibility of sensors

Although the superior sensitivity of graphene superhydrophobic sensor has been presented, it is crucial to analyze reversibility of the electrical response [9, 10]. With this purpose, the cyclic stretch-release test was performed. As shown in Fig. S7, the  $\Delta R/R_0$  of the graphene superhydrophobic sensor maintained very stable in the ten cycles of the cyclic stretching-releasing test at both 10% (Fig. S7a) and 20% strain (Fig. S7b), indicating the long working life and reversibility of the presented graphene sensors.

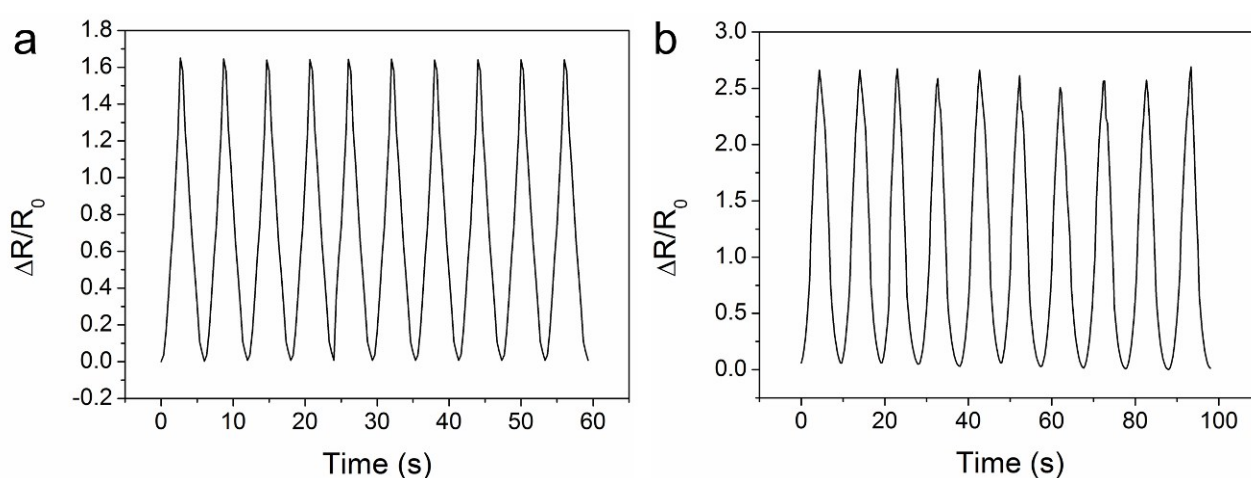


**Figure S7. Electrical response of the graphene composite during 10 cycles with settled maximum strain: (a) 10% and (b) 20%.**

### S8 Response time

The response time of the sensor is another crucial factor. In this research, the response time was measured according to the method shown in reference 11. As shown in the inset of Fig. S8, this graphene superhydrophobic sensor shows immediate response time of  $\sim 330$  ms under tension condition, which was comparable with recent values of other nanocomposite sensors (300-3800 ms) [11, 12]

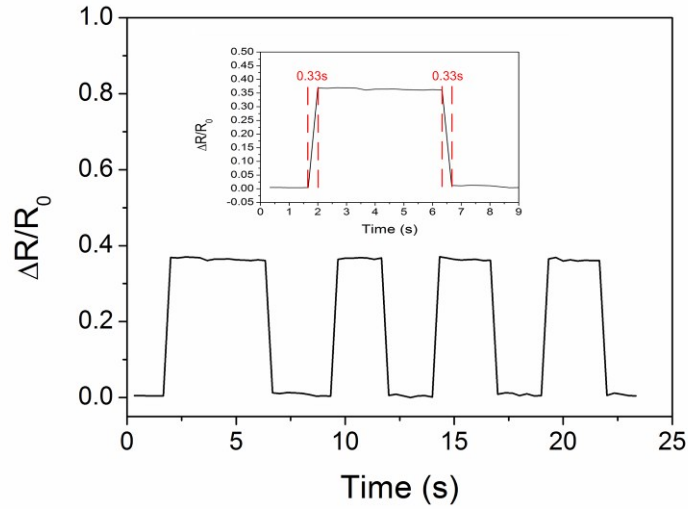


**Figure S8. Electrical response of the graphene composite that was subjected to periodic tensile force The inset is one enlarged peak showing the rise-time.**

### S9 Profilometer measurement

The surface roughness of the sample was further assessed using the Profilometer (Dektak XT). From the Figure S9a-e and Table S1, it can be found that the surface roughness become smoother as the strain of the graphene composited afforded become larger.

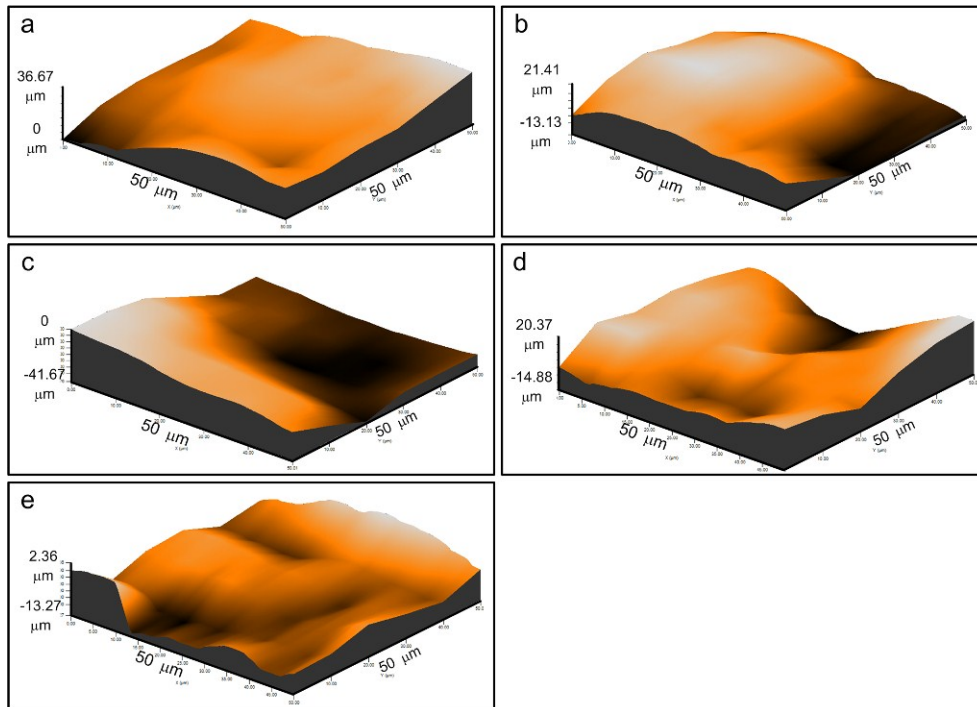


**Figure S8. The Profilometer images of graphene composite at strain of 0% (a), 100% (b), 200% (c), 300% (d) and 400% (e).**

**Table S1 The surface roughness of the graphene composite under different strains.**

Strain (%)	Roughness ( $\mu\text{m}$ )
0	5.22
100	4.28
200	3.99
300	3.31
400	1.93

**S10** The mechanism of water repellency after oil contamination

Nature is a ‘Top univeristy’ in the world and researchers can learn there for free. One of the fascinating branches of nature is the superhydrophobicity of lotus leaves. Inspired by the lotus leaves, the graphene superhydrophobic composite was prepared in this research (Fig. S10a). Another fascinating branch of nature is the slippery surface from *Nepenthes* pitcher plant, which use them to lock-in an intermediary liquid that then acts by itself as the repellent surface [13]. When the graphene superhydrophobic composite was immersed in oil, the oil gradually penetrated into the surface and then worked as a lubricating fluid (Fig. S10b). Due to dual supporting by both lubricating fluid and inherent superhydrophobicity, water droplets still remained marble-shaped [14].

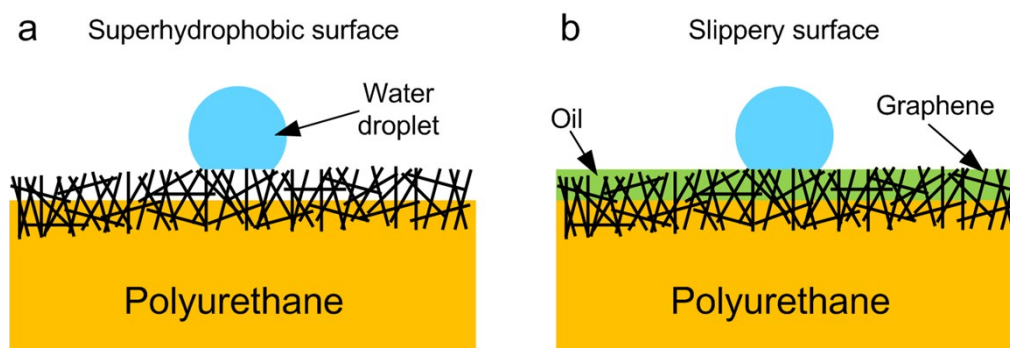


**Figure S10. The schematic of superhydrophobic surface (a) and slippery surface (b).**

**Supplementary References**

1. B. J. Basu, V. D. Kumar, C. Anadan, Surface studies on superhydrophobic and oleophobic polydimethylsiloxane-silica nanocomposite coating system. *Appl. Surf. Sci.*, 2012, **261**, 807.
2. N. Saleema, D. K. Sarkar, D. Gallant, R. W. Paynter, X. G. Chen, Chemical nature of superhydrophobic aluminum alloy surfaces produced via a one-step process using fluoroalkylsilane in a base medium. *ACS Appl. Mater. Interfaces*, 2011, **3**, 4775.

3. R. V. Lakshmi, P. Bera, C. Anandan, B. J. Basu, Effect of the size of silica nanoparticles on wettability and surface chemistry of sol-gel superhydrophobic and oleophobic nanocomposite coating. *Appl. Surf. Sci.*, 2014, **320**, 780.
4. R. Campostrini, M. Ischia, G. Carturan, Sol-gel synthesis and pyrolysis study of oxyfluoride silica gels. *J. Sol Gel Sci. Technol.*, 2002, **107**, 2.
5. L. J. Ward, W. C. E. Schofield, J. P. S. Badyal, A. J. Goodwin, P. J. Merlin, Atmospheric pressure glow discharge deposition of polysiloxane and SiO<sub>x</sub> films. *Langmuir*, 2003, **19**, 2110.
6. D. Pleul, R. Frenzel, M. Eschner, F. Simon, X-ray photoelectron spectroscopy for detection of the different Si-O bonding states of silicon. *Anal. Bioanal. Chem.*, 2003, **375**, 1276.
7. Y. Lee, Synthesis and properties of fluorinated carbon materials. *J. Fluorine Chem.*, 2007, **128**, 392.
8. H. Wang, J. Fang, T. Cheng, J. Ding, L. Qu, L. Dai, X. Wang, T. Lin, One-step coating of fluoro-containing silica nanoparticles for universal generation of surface superhydrophobicity. *Chem. Comm.*, 2008, **877**, 877.
9. L. Li, T. Hu, H. Sun, J. Zhang, A. Wang, Pressure-sensitive and conductive carbon aerogels from poplars catkins for selective oil absorption and oil/water separation. *ACS Appl. Mater. Interfaces*, 2017, **9**, 18001.
10. L. Li, B. Li, H. Sun, J. Zhang, Compressible and conductive carbon aerogels from waste paper with exceptional performance for oil/water separation. *J. Mater. Chem. A*, 2017, **5**, 14858.
11. K. Sun, J. Qi, Q. Zhang, Y. Yang, Y. Zhang, A novel logic switch based on individual ZnO nanotetrapods, *Nanoscale*, 2011, **3**, 2166.
12. Z. Wang, J. Qi, X. Yan, Q. Zhang, Q. Wang, S. Lu, P. Lin, Q. Liao, Z. Zhang, Y. Zhang, A self-powered strain sensor based on a ZnO/PEDOT:PSS hybrid structure, *RSC Adv.*, 2013, **3**, 17011.
13. T. Wong, S. H. Kang, S. K. Y. Tang, E. J. Smythe, B. D. Hatton, A. Grinthal, J. Aizenberg, Bioinspired self-repairing slippery surfaces with pressure-stable omniphobicity. *Nature*, 2011,

477, 443.

14. B. Chen, J. Qiu, E. Sakai, N. Kanazawa, R. Liang, H. Feng, Robust and superhydrophobic surface modification by a “paint +adhesive” method: applications in self-cleaning after oil contamination and oil-water separation. *ACS Appl. Mater. Interfaces*, 2016, **8**, 17659.